INJECTION LOSSES IN THE SOLEIL II STORAGE RING: SENSITIVITY TO BOOSTER AND TRANSFER LINE ERRORS

S. Habet*, A. Loulergue, L. S. Nadolski, M.-A. Tordeux
Synchrotron SOLEIL, Saint-Aubin, France

Abstract

Injection losses are a key challenge for SOLEIL II commissioning because the reduced storage-ring acceptance makes off-axis injection highly sensitive to transport and optics errors. We use multiparticle tracking with a corrected lattice model including realistic static and jitter errors in the booster and Transfer Line 2 (TL2). The results show that losses are primarily governed by the injected phase-space distribution at the Multipole Injection Kickers (MIK). Most particles are intercepted at the septum and at Straight Section 7 (SDM07), while the injection acceptance window sets the efficiency for all studied error scenarios. Emittance exchange improves the horizontal footprint only if the final TL2 focusing errors remain at the percent level; otherwise, the enlarged vertical beam size samples the non-linear MIK field and generates large horizontal over-kicks. These results provide practical tolerances and tuning priorities for top-up commissioning.

INTRODUCTION

The upgrade of the SOLEIL synchrotron to the 4th-generation light source SOLEIL II relies on a Multi-Bend Achromat lattice to reach ultra-low emittance and high photon brightness. This strong focusing, however, reduces the dynamic aperture and momentum acceptance of the Storage Ring (SR), making high-efficiency top-up injection one of the main challenges for commissioning and routine operation [1].

In the baseline scheme, beam injection is performed with an array of five Multipole Injection Kickers (MIKs) [2, 4, 6]. The beam extracted from the booster, with nominal emittances of 5 nm rad horizontally and 0.5 nm rad vertically, is transported through the TL2 and must be injected within the narrow SR acceptance. In practice, static and systematic errors in the booster and transfer line distort the beam phase space and can drive the injected distribution outside the accepted region, leading to localized losses. This paper presents multiparticle tracking simulations used to identify and quantify these loss mechanisms.

INJECTION SCHEME AND ERROR MODELING

To simulate the injection process under realistic machine conditions, a multiparticle tracking approach was employed, including realistic static and dynamic (jitter) errors in the booster and TL2, as summarized in Table 1.

* sami.habet@synchrotron-soleil.fr

Table 1: Static and dynamic errors in the booster and TL2. Inj.: injection; Extr.: extraction; PS: power supply.

Type	Source	RMS	Comment
Static	TL2 final triplet focusing	1%	Predominant error.
	Pulsed magnet field (LPM)	4.7×10^{-4}	LPM train length effect.
	TL2 quadrupole roll	0.2 mrad	Isolates coupling sources.
	Inj./extr. magnet roll	0.05 mrad	Residual orbit imperfections.
Jitter	Pulsed magnet amplitude	2×10^{-4}	Pessimistic worst-case.
	Booster extracted beam	H: 20 μm, 2.5 μrad V: 2 μm, 1 μrad	Booster PS tracking error (5×10^{-5}).

MULTIPARTICLE TRACKING AND PHASE-SPACE ANALYSIS

To model the beam dynamics, multiparticle tracking simulations were performed using the Accelerator Toolbox (AT) [7] framework. After tracking the distributions through the TL2, they are injected at the middle of the storage ring straight injection section. The storage ring lattice model includes realistic alignment offsets and multipole errors, quantitatively detailed in Ref. [3], which have been virtually corrected using standard operational procedures (orbit correction, BBA, and LOCO).

To fully assess the injection efficiency and complement the global commissioning start-to-end simulations reported in Ref. [3], the particles are tracked over 1000 turns. This tracking duration covers about 2.1 synchrotron periods ($Q_s \approx 0.00209$), which is sufficient to probe the dominant early losses associated with longitudinal mismatch and transverse acceptance limitations, and to estimate the injection capture rate. During the first turn, the MIK field is turned on to simulate the off-axis injection kick. For all subsequent turns, the MIK is turned off and becomes transparent. To accurately reproduce the complex non-linear dynamics induced by the MIK, a thick-lens tracking approach is implemented. The MIK is sliced into small longitudinal steps ds. At each step, the 2D magnetic field maps $B_y(x, y)$ and $B_x(x, y)$—normalized per kiloampere—are interpolated at the exact transverse coordinates of each macro-particle. The

angular kicks imparted over a slice ds are computed as:

$$\Delta x' = \frac{I_{\mathrm{MIK}} \cdot B_y(x,y)}{B\rho(1+\delta)} ds$$
$$\Delta y' = \frac{I_{\mathrm{MIK}} \cdot B_x(x,y)}{B\rho(1+\delta)} ds \quad (1)$$

where I_{MIK} is the kicker current, $B\rho$ is the magnetic rigidity, and $\delta = \Delta p/p_0$. Positions are then advanced assuming a simple drift over ds, ensuring off-axis particles correctly sample the field variations.

To optimize the injection parameters, a preliminary 2D scan of the injected beam centroid coordinates was performed over a horizontal position range of $x \in [-7, -3]$ mm and an angle range of $x'_0 \in [0, 1.3]$ mrad. This scan generated the injection efficiency chart (Fig. 1), which clearly maps the 100% efficiency acceptance zone of the storage ring. Based on this map, the transfer line optics and steering were tuned to perfectly center the centroids (i.e., the center of each bunch) of the 1000 simulated bunches directly into the core of this optimal zone.

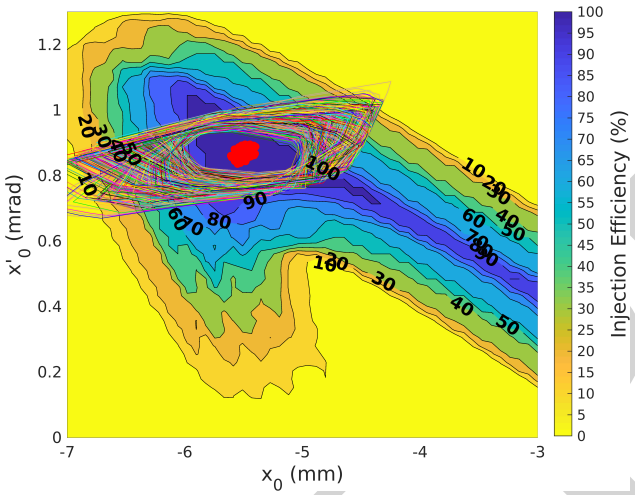

Figure 1: Injection efficiency chart. The centroids of the 1000 simulated bunches (red dots) are matched to the 100% injection efficiency zone; the colored ellipses indicate the maximum extent of each bunch.

However, even when the bunch centroids are correctly centered in the 100% injection-efficiency region (red dots), accumulated static and dynamic errors from the booster and the TL2 (Table 1) broaden the phase-space distribution and drive the bunch tails beyond the acceptance region. The resulting longitudinal loss map is shown in Fig. 2. For the 1% focusing-error case (red), about 70% of the losses occur at the injection septum (−5 mm from the closed orbit), while about 20% are observed at SDM07. In contrast, for the 5% case (blue), the loss probability becomes much higher in the first sections of the ring, and the total number of lost particles increases from about 25 to 3×10^4.

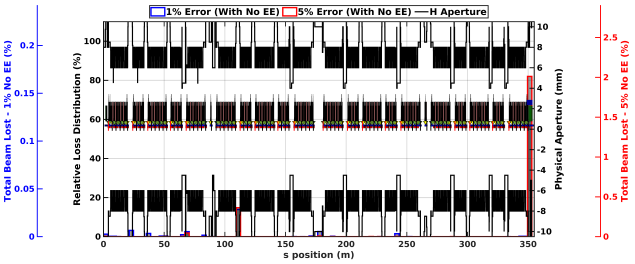

Figure 2: Loss distribution in the horizontal plane along the SOLEIL II storage ring for two quadrupole focusing error configurations: red, 1%; blue, 5%. For the 1% case, losses are mainly localized at the septum and at SDM07, whereas the 5% case shows higher loss probabilities in the first sections of the ring.

EMITTANCE EXCHANGE SENSITIVITY TO TRANSFER LINE OPTICS

Emittance exchange (EE) [5] has been proposed as a possible strategy to reduce injection losses in the horizontal plane. Its benefit, however, depends strongly on tight control of the vertical beam envelope at injection.

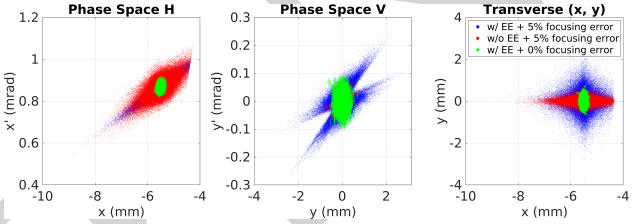

Figure 3: Phase-space distributions for three cases: with EE and 0% focusing error (green), with EE and 5% focusing error (blue), and without EE with 5% focusing error (red).

To quantify this sensitivity, multiple static gradient errors were introduced into the final focusing elements of the transfer line. Simulations show that the EE scheme remains efficient only when the relative focusing error on these final quadrupoles is kept below the 1% level. The main effect of this sensitivity is illustrated in Fig. 3. For the 0% EE case (green), the horizontal phase-space footprint is reduced while the vertical beam size remains within acceptable bounds ($\pm$1 mm). In contrast, for the 5% EE case (blue), the vertical phase space undergoes a strong blow-up, with a large horizontal phase space and cancels the benefit of emittance exchange. The case without EE at 5% (red) shows that the horizontal phase space remains comparable to that obtained with EE under the same degraded focusing conditions.

The consequence of this degradation is visible in the longitudinal loss distribution along the storage ring (Fig. 4). Comparing the two EE cases (optimistic 1% vs. pessimistic 5%) shows that the 5% case (blue) generates significantly higher losses than the 1% case (red). This confirms that the vertical blow-up directly increases losses in the horizontal plane.

To explain this behavior, we examine the MIK field topology (Fig. 5). At the injected horizontal offset, $x \approx -3.5$ mm, the vertical field component varies strongly with the vertical

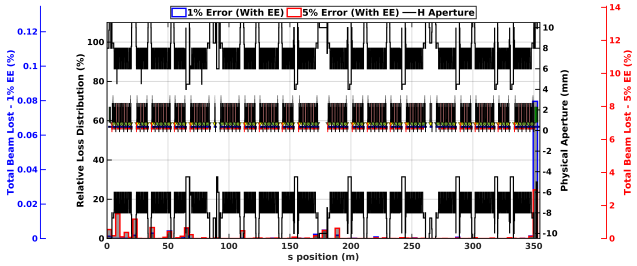

Figure 4: Loss identification along the storage ring for two emittance-exchange cases: 1% focusing error (red) and 5% focusing error (blue).

coordinate y. Particles close to $y = 0$ receive the nominal kick, whereas particles at large vertical amplitudes sample a much stronger field. In the 5% EE case, the vertical beam size expands to several millimeters, and part of the beam therefore receives a strong horizontal over-kick. This non-linear effect explains the horizontal blow-up observed in Fig. 6 and the associated losses.

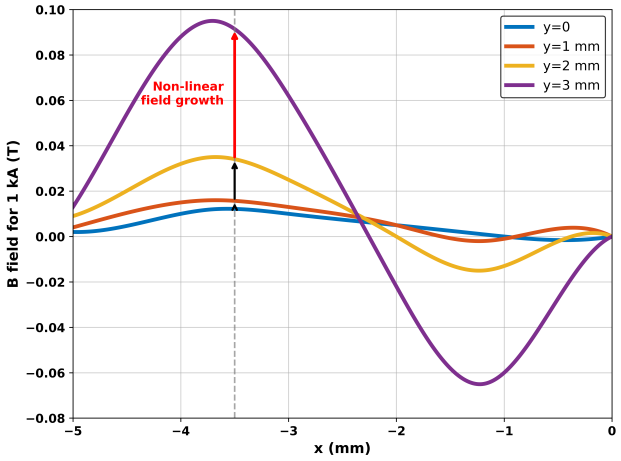

Figure 5: MIK vertical magnetic field (B_y) profile as a function of the horizontal coordinate (x) for different vertical displacements (y).

To better isolate this non-linear kick, a back-tracking computation was performed (Fig. 6). The red markers show the particle coordinates back-tracked to the injection point using a pure negative drift, effectively subtracting the MIK field. The resulting distribution exhibits a strong horizontal blow-up, confirming that the vertically enlarged beam samples the non-linear MIK field and receives large horizontal kicks. Many particles are therefore driven outside both the ideal and corrected dynamic aperture, leading to substantial beam losses.

CONCLUSION

In this paper, tracking simulations under realistic error conditions demonstrate that high-efficiency injection for SOLEIL II relies fundamentally on stringent control of the TL2 optics. As long as the transfer line is finely tuned (focusing errors below 1%), the injected bunch centroids can be matched to the core of the 100% efficiency acceptance

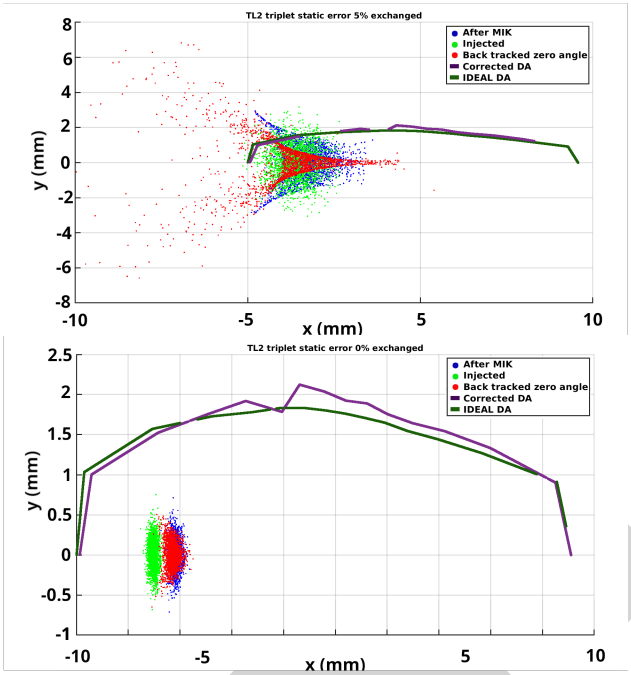

Figure 6: Transverse particle distributions at injection for a 5% (top) and a 0% (bottom) static focusing error on the TL2 final triplet, compared to the storage ring dynamic aperture (DA). Green: injected distribution; Blue: after tracking through the MIK; Red: back-tracked without the MIK effect.

zone, keeping localized losses at the septum and SDM07 low.

Consequently, our analysis does not show a clear operational benefit from applying emittance exchange (EE) prior to injection. If TL2 is properly tuned, standard injection is already highly efficient. Conversely, if the optics are degraded, the EE scheme causes a severe vertical beam blow-up. Due to the highly non-linear MIK magnetic field, this vertical expansion generates large horizontal over-kicks that push particles outside the dynamic aperture, ultimately increasing total losses. Operationally, the required <1% tolerance on the standard optics should be understood as an effective matching target, achievable through empirical quadrupole tuning based on the measured injected beam footprint and transmission. Mastering this standard tuning is therefore the safest and most robust strategy.

REFERENCES

[1] A. Loulergue *et al.*, "SOLEIL II Conceptual Design Report", Synchrotron SOLEIL, Saint-Aubin, France, 2021.

[2] M.-A. Tordeux *et al.*, "Injection Schemes for the SOLEIL Upgrade", in *Proc. IPAC'21*, Campinas, SP, Brazil, May 2021, paper MOPAB248. doi:10.18429/JACoW-IPAC2021-MOPAB248

[3] S. Habet *et al.*, "Start to end commissioning simulations for SOLEIL II storage ring", in *Proc. IPAC'25*, Taipei, Taiwan, Jun. 2025, paper MOPS040. doi:10.18429/JACoW-IPAC2025-MOPS040

[4] R. Ollier *et al.*, "Toward transparent injection with a multipole injection kicker in a storage ring", *Phys. Rev. Accel. Beams*, vol. 26, no. 2, p. 020101, 2023. doi:10.1103/PhysRevAccelBeams.26.020101

[5] P. Schreiber *et al.*, "SOLEIL II booster robustness and emittance exchange", in *Proc. IPAC'24*, Nashville, TN, USA, May 2024, paper THPC36. doi:10.18429/JACoW-IPAC2024-THPC36

[6] P. Alexandre *et al.*, "Transparent Top-Up Injection into Fourth-Generation Storage Ring", *Nucl. Instrum. Methods Phys. Res., Sect. A*, vol. 986, p. 164739, 2021. doi:10.1016/j.nima.2020.164739

[7] B. Nash *et al.*, "New Functionality for Beam Dynamics in Accelerator Toolbox (AT)", in *Proc. IPAC'15*, Richmond, VA, USA, May 2015, pp. 113-115.